

METHOD FOR CALCULATING THE INSTRUMENT FUNCTION OF A MEDICAL HYPERSPECTROMETER

V.I. Zavarzin

zavarzin@bmstu.ru

Bauman Moscow State Technical University, Moscow, Russian Federation

Abstract

Hyperspectral imaging technology offers great opportunities in noninvasive disease diagnostics and scientific research. Medical hyperspectrometer operation is based on the light ability to be reflected from biological tissue and depends on how strongly the tissue absorbs/reflects the light. Knowledge of the reflected and scattered light from tissues makes it possible to accurately interpret the state of health of a patient. Hyperspectrometer was considered consisting of projection lens that takes a picture of the patient's body from the finite distance, imaging spectrometer, as well as of calibrated radiation sources to illuminate the areas under study. Image decomposition into spectrum was implemented in the scheme of a classical spectrometer, which entrance slit was the exposure slit of the imaging lens. To ensure scanning, it was supposed to use displacement either of the spectrometer or of the patients under examination on a conveyor belt. A technique is proposed for determining the instrument function of a medical hyperspectrometer taking into account the scattering function influence of optical system, slit, optical radiation receiver, image displacement relative to the slit and electronics. By analyzing the instrument function, it becomes possible to implement various methods for assessing the optical image quality, such as modulation transfer function and spatial and spectral resolution, which is required for correct use of the device and image interpretation. The instrument design process involves optimization of the main circuit and design solutions according to the criterion of their influence on the instrument function and the generated image quality. An example of instrument design was considered involving optimization of the basic circuitry and design solutions

Keywords

Lens, spectrometer, instrument function, Fourier transform, data hypercube

Received 19.03.2022

Accepted 19.05.2022

© Author(s), 2022

Introduction. Significant success was achieved in the recent years in mastering the optical range of the electromagnetic oscillations spectrum. Modern optical radiation sources and receivers were developed, and they created the basis for new hyperspectral optoelectronic devices used in scientific research, industry, agriculture, etc. Spectral instruments are the unique means in studying the surrounding objects covering a spectral interval ten times wider than the human eye. Each solid, liquid or gaseous object has its own unique spectral “portrait” characterizing its chemical composition, state and thus identifying the object under study. The most common task of hyperspectral measurements in the optical range of 0.3–2.5 μm includes the Earth remote sensing, product quality and safety control, research in archeology and art, as well as in forensic science [1–5]. Achievements in the element base of the optoelectronic instrumentation and image formation and analysis in the ultraviolet, visible and infrared spectral regions made them attractive for using in the medical research [6–14]. Hyperspectral imaging technology is holding significant promise in the non-invasive disease diagnostics and scientific research. Medical hyperspectral device (MHSD) differs, for example, from hyperspectral equipment for the Earth remote sensing [1, 15] in its equipment that includes the projection lens filming from a finite distance, as well as in using the calibrated radiation sources to illuminate the samples under study. To ensure scanning, displacement of the studied patients or of the MHSD on a conveyor belt is usually used.

The light ability to be reflected from biological tissue depends on how strongly it absorbs the light [10–12]. In turn, absorption is a function of the molecular composition. Thus, for example, absorption coefficient at the wavelength of 660 nm is 0.053 for a leg, blood-saturated 1.3, and oxygen-deprived is 4.9 cm^{-1} . The diseased state of tissues leads to a corresponding alteration in their reflective properties. Thus, knowledge of reflected and scattered light makes it possible to accurately interpret measurement data on the state of the tissue [14].

Transition from multi-zone imaging to the hyperspectral imaging increases not only the information amount, but also provides completely new great opportunities to extract information on the state of the object under study. Only hyperspectral measurements are able to reveal small spectral differences between separate elements of the body surface and serve as an indicator of the disease processes being of interest to specialists. However, these data could be extracted only with correct use of the equipment and interpretation of the obtained images, which requires knowledge of the real hyperspectrometer characteristics.

Problem statement. The process of receiving and processing optical radiation envisages introducing various instrumental distortions, which could be mathematically simulated as the instrument function and taken into account

when determining the hyperspectrometer characteristics and, first of all, its spectral and spatial resolution. Using the MHSD instrument function at the stages of design, optimization of the design solutions, as well as assembly, calibration and evaluating quality of the finished equipment would make it possible to use the device correctly and improve the quality of image interpretation.

Problem solution. Medical hyperspectral device consists of an imaging lens (IL) and the image spectrometer, where the spectrometer entrance slit is located in the IL image plane (Fig. 1). The slit is oriented across the equipment platform motion direction with the angular field limited by the lock range. Using the spectrometer, the image slice with the exit slit spectral resolution is output to the receiver.

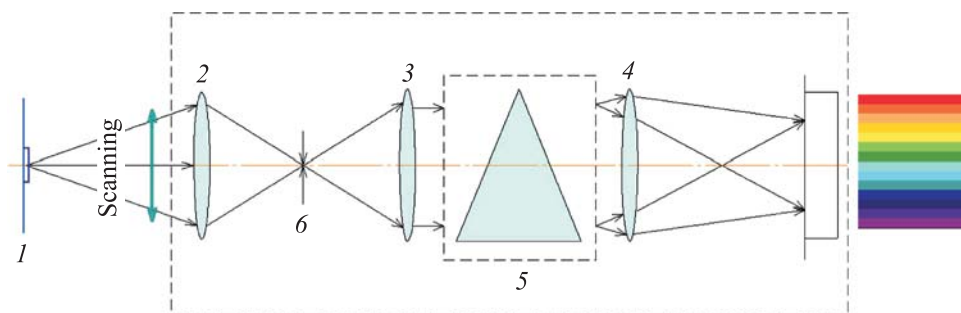


Fig. 1. Hyperspectral device operation scheme:

1 is test sample; 2 is IL; 3 is collimating lens; 4 is fixing lens; 5 is dispersing device;
6 is entrance slit

Image decomposition into a spectrum is implemented in the scheme of a classical spectrometer, which entrance slit is the IL exposure slit. The system is built according to the following principle: the IL films from the finite distance and forms the image of the filming object moving perpendicular to the optical axis on a slit installed in the IL image plane. The slit width is equal to the size of the image receiver element, and is determined by the line direction according to the MHSD capture requirement.

The collimating lens collimates beams of rays from the image onto the slits and directs the parallel beam of rays to a dispersing device (DD). The image of the object under study moving along the slit is decomposed on the DD into a spectrum, which is focused by the lens on the image receiver. In this case, space is depicted in the receiver line direction, and the slit image moving spectrum is depicted in the column direction. Both the reflective diffraction grating and the prism systems, including those in the autocollimation mode, could be used as the DD [15]. Hyperspectrometers with the DD have high spatial and spectral resolution. However, it should not be forgotten that DD and scanning

complicate the design, increase the manufacturing complexity, increase the equipment weight and size parameters and tighten requirements to the operating conditions.

The two-dimensional matrix is the receiver. In the first dimension parallel to the slit, the image cut by the slit and generated by the IL is displayed along the receiver line, while in the second dimension perpendicular to the slit, the image is spectrally scanned. Spatial information in the transverse direction is accumulated due to scanning and is carried out by displacing along the object under study (Fig. 2). Thus, a three-dimensional data hypercube is formed that includes spectral information of each pixel of the patient under study. Data hypercube (DHC) is understood as a set of images of the same subject of the patient's body obtained simultaneously in a variety of narrow spectral ranges (channels).

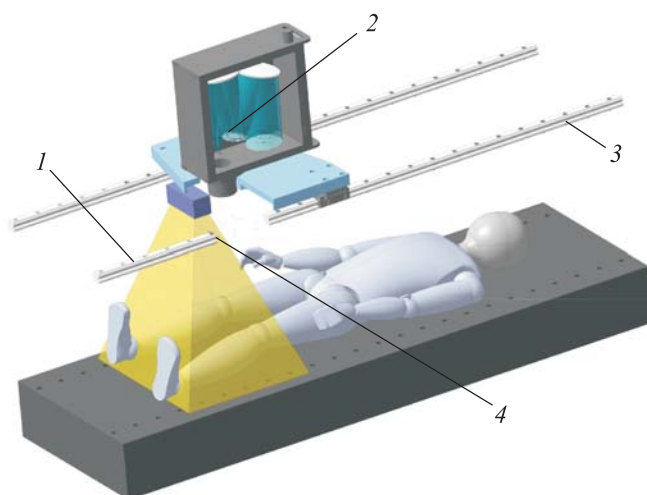


Fig. 2. Experimental MHSD external appearance:
1 is radiation source; 2 is spectrometer; 3 is guides; 4 is IL

Using DHC obtained in a short period of time and MHSD, easily and quickly the following problems could be solved: spectral analysis of the human body itself (open wounds, tumors), mixed structures study, spectral characteristic of each point of the sample under study localization, prompt tracking the course of various processes, etc. In addition, equipment setup is facilitated by visual control of the resulting images.

The hardware design process involves optimization of the main circuitry and design solutions according to the criterion of their influence on the formed image quality (its optotechnical parameters). The image obtained with a spectral instrument is not an absolute copy of the shooting scene image, since fine details

of the objects are blurred. This blurring size is determined by the general scattering function, which is also called the $A(x, y)$ device instrument function.

By analyzing the instrument function, several methods for assessing the optical image quality could be implemented, such as modulation transfer function (MTF), spatial resolution and spectral resolution. With the ideal optical design, DD, radiation receiver and electronics, the radiation detector pixel size would determine the spatial and spectral resolution. However, components of a hyperspectral instrument in real conditions introduce distortions; therefore, spectral and spatial resolution should be simulated at the design stage.

The object optical radiation could be described using spectral distribution of the object brightness. Optical system within the framework of the diffraction scalar theory is a spatial filter, which is characterized by the optical transfer function. As a result of transformations in the optical system, we have the illumination spectral distribution at the exit.

It is customary to evaluate image quality at the characteristic frequency equal to $2/3$ of the Nyquist frequency. According to the Kotelnikov theorem, only frequencies below the Nyquist frequency would carry useful information at signal sampling. The Nyquist frequency is $1/(2d)$, where d is the matrix pixel size. It is necessary to ensure coordinated operation of the lens with the low-pass filter and the image receiver that the MTF value is equal to 0.4 at the characteristic frequency. In the case when the low-pass filter is missing in the optical system, its role should be played by the optical system itself. In this case, the MTF at this frequency should be 0.16.

To analyze the MHSD quality, the output signal could generally be represented as convolution of the $I_0(x, y)$ input signal and the instrument function [16, 17]:

$$I(w, r) = \iint_W I_0(x, y)A(w-x, r-y) dx dy,$$

where $A(w-x, r-y)$ is the device response shifted by w and r values; W is the range of coordinates, where the device response is significant.

In spectral devices, each separate λ wavelength corresponds to a certain y coordinate in the focal plane, in which direction information about spectral composition of the detected radiation is located. Thus, instrument function along the OY -axis could be written in the $A(x, \lambda)$ form for each fixed λ , and it will be called the spectral instrument function.

The instrument function for MHSD is the following convolution:

$$A_{gen}(x, y) = \text{PSF}_{opt} \text{PSF}_{sl} \text{PSF}_{rec} \text{PSF}_{sc} \text{PSF}_{el},$$

where PSF_{opt} is the optical scattering function; PSF_{sl} is the function that takes into account the slit effect on the total scattering function; PSF_{rec} is the function that takes into account the radiation receiver influence; PSF_{sc} is the scattering function connected to image displacement relative to the slit; PSF_{el} is the function that takes into account the influence of electronics.

Point scattering optical function. The optical system is never “ideal”; therefore, the energy from the source is scattering and distributing in the IL image plane within a certain small area. The point scattering function (PSF) is defined as the spatial energy distribution of illumination in the point source image. The scattering degree depends on many factors, including diffraction, aberrations and quality of the optical system mechanical assembly.

The optical PSF_{opt} could be described with satisfactory accuracy by the two-dimensional.

Gaussian function [16] $PSF_{opt}(x, y) = \exp(-x^2 / a^2) \exp(-y^2 / b^2)$, where a and b are the coefficients calculated based on requirements to the PSF half-width,

$$a = \sqrt{-\frac{\delta_x^2}{4 \ln 0.5}}; \quad b = \sqrt{-\frac{\delta_y^2}{4 \ln 0.5}},$$

δ_x, δ_y are the optical PSF half-width defined as the function width at the level of half of its maximum value along the x and y axes, respectively.

To find the optical transfer function, let us apply the Fourier transform to the scattering function:

$$TF_{opt}(v_x, v_y) = \exp(-\pi^2 a^2 v_x^2) \exp(-\pi^2 a^2 v_y^2),$$

where v_x, v_y is the spatial frequency.

If the optical system design parameters are known, the expected (calculated) value of the optical PSF could be obtained with high accuracy by simulating in programs for the optical system automated calculation.

This approach disadvantage is that it does not consider the influence on the optical system image quality of such factors as striations and inhomogeneities of optical materials; defects of optical surfaces and coatings; optics contamination during operation; light scattering, glare, etc.

The function that takes into account the slit effect on the overall PSF describes spatial blurring associated with the finite size of the hyperspectral equipment entrance slit. This influence manifests itself in the case of an imaging spectrometer built on the DD basis. Such entrance slit influence function has the following form:

$$\text{PSF}_{sl}(y) = \text{rect}(y/h),$$

where h is the slit width. Fourier transform from this function is

$$\text{TF}_{sl}(v_y) = \text{sinc}(\pi h v_y).$$

In the case an image of an insignificant part of the patient's body surface is needed, it is possible to build a spectrometer without a slit, DD and without scanning. In this case, additional optical filters should be introduced into the optical system, and additional mathematical processing of the obtained images should be provided.

The function that considers the radiation receiver influence describes spatial blurring associated with non-zero sizes of the receiver sensitive elements. The function has the following form:

$$\text{PSF}_{rec}(x, y) = \text{rect}(x/d_x) \text{rect}(y/d_y),$$

where d_x is the size of the image receiver element across the route (along the line); d_y is the size of the image receiver element along the route (along the column).

Receiver element transfer function in the frequency domain is as follows:

$$\text{TF}_{rec}(v_x, v_y) = \text{sinc}(\pi d_x v_x) \text{sinc}(\pi d_y v_y).$$

The matrix receiver mathematical model is based on the fact that the receiver converts a two-dimensional optical signal into the one-dimensional electrical video signal $u(t)$, where t is the time coordinate. Due to the fact that continuous illumination distribution is converted by the matrix receiver into the discrete charge distribution signal, the sampling imaging system turns out to be spatially non-invariant, i.e., the image of a point source depends on its position relative to the two-dimensional lattice of the matrix (sampling). If certain requirements and assumptions are met, fundamental approach to the imaging system analysis based on the theory of linear spatial filtering and the use of the modulation transfer function could be extended to such systems.

The scattering function associated with the image displacement relative to the slit takes into account the image blurring that occurs, if during the time that the signal for a given pixel is being integrated, the image is shifted from one detecting element to another. This shift is simulated using a one-dimensional PSF having the form of a rectangular pulse $\text{PSF}_c(y) = \text{rect}(y/s)$, where s is the spatial image blurring in the IL image plane defined as the image shift expressed in pixel fractions during the integration time.

After the Fourier transform from the image displacement function, the following is obtained:

$$TF_{sc}(v_y) = \text{sinc}(\pi s v_y).$$

The equipment electronic path during accumulation and transfer of charges, signal digitization and its amplification causes distortions affecting the instrument function. In each case, the function that considers the influence of electronics is calculated separately or measured.

To calculate the instrument function, it is necessary to determine the general transfer function. Applying the convolution theorem, it becomes possible to obtain it as the product of their Fourier transforms of all transfer functions of the scattering function main elements [15, 16]:

$$TF_{gen}(v_x, v_y) = TF_{opt} TF_{sl} TF_{rec} TF_{sc} TF_{el}.$$

A feature of the hyperspectral equipment operation is the instrument function separation into the longitudinal ($A_{||}(y)$) and transverse ($A_{\perp}(x)$) components. Spatial characteristics of the filming scene are measured in the longitudinal component direction, and information is obtained in the transverse direction on the image spectral composition of the patient's body limited by the spectrometer entrance slit:

$$\begin{aligned} TF_{gen}(v_x) &= \exp(-\pi^2 a^2 v_x^2) \text{sinc}(\pi d_x v_x); \\ TF_{gen}(v_y) &= \exp(-\pi^2 b^2 v_y^2) \text{sinc}(\pi h v_y) \text{sinc}(\pi d_y v_y) \text{sinc}(\pi s v_y). \end{aligned} \quad (1)$$

The transfer function amplitude component, i.e., MTF, is of greatest interest in evaluating the image quality. Entering the MTF designation, the following expression is obtained:

$$MTF_{gen} = |TF_{gen}| = MTF_{opt} MTF_{sl} MTF_{rec} MTF_{sc} MTF_{el}. \quad (2)$$

Applying the inverse Fourier transform to the general transfer function, the formula for calculating the instrument function could be obtained:

$$A_{gen}(x) = \tilde{F}^{-1}(TF_{gen}(v_x)); \quad A_{gen}(y) = \tilde{F}^{-1}(TF_{gen}(v_y)), \quad (3)$$

where \tilde{F}^{-1} is the inverse Fourier transform operator.

Example. Let us determine characteristics of the hyperspectral equipment. Let the equipment operate in the range of 1.1–2.2 μm with spectral resolution of 3–20 nm. The transfer function simulation parameters are as follows: for the radiation receiver — a matrix with element dimensions of 24 \times 32 μm ; spectrometer entrance slit width is 24 μm ; optical PSF half-width value is $\delta_x = \delta_y = 14.35 \mu\text{m}$. The electronics PSF and image motion influence on the general function was not taken into account.

Using expressions (1)–(3), a graph of the instrument function in the longitudinal and transverse directions is obtained (Fig. 3).

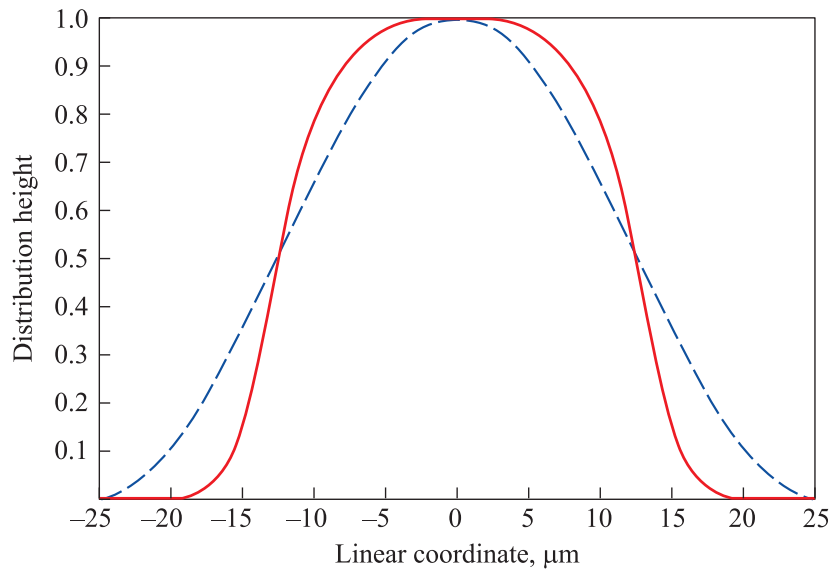


Fig. 3. Calculated instrument function in the longitudinal (dashed) and transverse (solid) directions

By analyzing the graphs, the linear size of the instrument function distribution cross section could be obtained at any level of the scattering distribution height. In this case, the spectral instrument function width is $\Delta y(\lambda) = 26 \mu\text{m}$ the level of 50 % of the distribution height.

Discussion of the obtained results. In the considered example, a fixed value of the optical PSF half-width $\delta_x = \delta_y = 14.35 \mu\text{m}$ was taken in the calculation; however, this value could significantly depend on the wavelength and on the angular field point in real devices. In this case, the instrument function should be calculated for each wavelength and field point separately [18, 19].

By analyzing the instrument function, it becomes possible to implement not only various methods in evaluating the device quality, but also to determine the influence of each element on this quality, also during assembly and calibration.

When creating photometric methods and devices for diagnosing the state of human health, it is important to understand both the process of the reflected electromagnetic wave formation and the features of the subsequent stages of data interpretation that form requirements to the equipment output data. Due to the large number of MHS spectral channels and complexity of solving the correct identification problem (in regard to the state of human health),

region for the problem under consideration. It is also necessary to create a database of spectral responses for various deviations and provide an automatic computerized procedure for processing the hyperspectral information and its interpretation.

At the stage of evaluating quality of the manufactured optical system, the inverse problem is of interest, i.e., restoring the optical system scattering function based on the known brightness distributions on the object and the illumination distribution at the receiver. This method makes it possible to calculate most of the image quality characteristics of the optical systems.

Conclusion. A technique is proposed to determine the MHSD instrument function having high spatial and spectral resolution. Based on the results of the analysis of the instrument function, it becomes possible to implement various methods for assessing the optical image quality using MTF, spatial and spectral resolution. This is necessary for the device correct operation and interpretation of images. Introduction of the developed methodology at the design stage would make it possible to determine the influence of various elements on the quality and optimize design solutions, which, in turn, would allow developing a MHSD with high characteristics, and their use in medical practice would ensure identification of various diseases at an early stage.

REFERENCES

- [1] Goetz A.F.H. Three decades of hyperspectral remote sensing of the Earth: a personal view. *Remote Sens. Environ.*, 2009, vol. 113, pp. 5–16.
DOI: <https://doi.org/10.1016/j.rse.2007.12.014>
- [2] Fischer C., Kakoulli I. Multispectral and hyperspectral imaging technologies in conservation: current research and potential applications. *Stud. Conserv.*, 2006, vol. 7, pp. 3–16. DOI: <https://doi.org/10.1179/sic.2006.51.Supplement-1.3>
- [3] Liang H. Advances in multispectral and hyperspectral imaging for archaeology and art conservation. *Appl. Phys. A*, 2012, vol. 106, no. 2, pp. 309–323.
DOI: <https://doi.org/10.1007/s00339-011-6689-1>
- [4] Gowen A.A., O'Donnell C.P., Cullen P.J., et al. Hyperspectral imaging — an emerging process analytical tool for food quality and safety control. *Trends Food Sc. Technol.*, 2007, vol. 18, no. 12, pp. 590–598. DOI: <https://doi.org/10.1016/j.tifs.2007.06.001>
- [5] Edelman G.J., Gaston E., van Leeuwen T.G., et al. Hyperspectral imaging for non-contact analysis of forensic traces. *Forensic Sc. Int.*, 2012, vol. 223, no. 1-3, pp. 28–39.
DOI: <https://doi.org/10.1016/j.forsciint.2012.09.012>
- [6] Carrasco O., Gomez R.B., Chainani A., et al. Hyperspectral imaging applied to medical diagnoses and food safety. *Proc. SPIE*, 2003, no. 5097, pp. 215–221.
DOI: <https://doi.org/10.1117/12.502589>

- [7] Afromowitz M.A., Callis J.B., Heimbach D.M., et al. Multispectral imaging of burn wounds: a new clinical instrument for evaluating burn depth. *IEEE Trans. Biomed. Eng.*, 1988, vol. 35, no. 10, pp. 842–850. DOI: <https://doi.org/10.1109/10.7291>
- [8] Wang L.V., Wu H.-I. Introduction in biomedical optics. Hoboken, Wiley, 2007.
- [9] Costas B., Christos P., George E. Multi/hyper-spectral imaging. In: Handbook of biomedical optics. Boca Raton, CRC Press, 2011, pp. 131–164.
- [10] Tuchin V.V., Tuchin V. Tissue optics. Bellingham, SPIE Press, 2007.
- [11] Pierce M.C., Schwarz R.A., Bhattar V.S., et al. Accuracy of *in vivo* multimodal optical imaging for detection of oral neoplasia. *Cancer Prev. Res.*, 2012, vol. 5, no. 6, pp. 801–809. DOI: <https://doi.org/10.1158/1940-6207.capr-11-0555>
- [12] Tuan V.-D. Optical properties of tissue. In: Biomedical photonics handbook. Boca Raton, CRC Press, 2003, pp. 1–76.
- [13] Welch A.J., Martin J.C., Star W.M. Definitions and overview of tissue optics. In: Optical-thermal response of laser-irradiated tissue. New York, Springer, 2011, pp. 27–64.
- [14] Lu G., Fei B. Medical hyperspectral imaging: a review. *J. Biomed. Opt.*, 2014, vol. 19, no. 1, art. 010901. DOI: <https://doi.org/10.1117/1.jbo.19.1.010901>
- [15] Zavarzin V.I., Li A.V. Instrument function design procedure of the hyper-spectral filming equipment for the Earth remote sensing. *Inzhenernyy zhurnal: nauka i innovatsii* [Engineering Journal: Science and Innovation], 2012, no. 9 (in Russ.). DOI: <https://doi.org/10.18698/2308-6033-2012-9-352>
- [16] Mosyagin G.M., Lebedev E.N., Nemtinov V.B. Teoriya optiko-elektronnykh system [Theory of optic-electronic systems]. Moscow, Mashinostroenie Publ., 1990.
- [17] Li A.V. Opticheskie sistemy malogabaritnoy giperspektralnoy apparatury distantsionnogo zondirovaniya Zemli iz kosmosa. Dis. kand. tekhn. nauk [Optical systems of small-size hyperspectrum equipment for Earth remote sensing. Cand. Sc. (Eng.). Diss.]. Moscow, Bauman MSTU, 2017 (in Russ.).
- [18] Zavarzin V.I., Li A.V. Performance calculations of hyperspectral instrument with prismatic dispersive device. *Herald of the Bauman Moscow State Technical University, Series Instrument Engineering*, 2015, no. 1 (100), pp. 111–120 (in Russ.). DOI: <https://doi.org/10.18698/0236-3933-2015-1-111-120>
- [19] Zavarzin V.I., Li A.V. [Hyperspectral medical device]. *Nauch.-tekhn. konf. "Mediko-tekhnicheskie tekhnologii na strazhe zdorovya"* [Proc. Sc.-Tech. Conf. Medical-Technical Technologies on Guard of Health]. Moscow, Bauman MSTU Publ., 2014, pp. 66–69.

Zavarzin V.I. — Dr. Sc. (Eng.), Professor, Department of Laser and Optoelectronic Systems, Dean of the Department of Optoelectronic Instrument Engineering, Bauman Moscow State Technical University (2-ya Baumanskaya ul. 5, str. 1, Moscow, 105005 Russian Federation).

Please cite this article as:

Zavarzin V.I. Method for calculating the instrument function of a medical hyperspectrometer. *Herald of the Bauman Moscow State Technical University, Series Instrument Engineering*, 2022, no. 3 (140), pp. 92–102. DOI: <https://doi.org/10.18698/0236-3933-2022-3-92-102>